

# First photometric study of ultrashort-period contact binary 1SWASP J140533.33+114639.1

Bin Zhang<sup>1,2,3</sup>, Sheng-bang Qian<sup>1,2,3</sup>, R. Michel<sup>4</sup>, B. Soonthornthum<sup>5</sup> and Li-ying Zhu<sup>1,2,3</sup>

<sup>1</sup> Yunnan Observatories, Chinese Academy of Sciences (CAS), P. O. Box 110, 650216 Kunming, China;  
*zhangbin@ynao.ac.cn*

<sup>2</sup> Key Laboratory of the Structure and Evolution of Celestial Objects, Chinese Academy of Sciences, P. O. Box 110, 650216 Kunming, China

<sup>3</sup> University of Chinese Academy of Sciences, Yuquan Road 19#, Sijingshang Block, 100049 Beijing, China

<sup>4</sup> Instituto de Astronomía, UNAM, Ensenada, México

<sup>5</sup> National Astronomical Research Institute of Thailand, 191 Siriphanich Bldg. 2nd Fl. Huay Kaew Rd. Suthep District, Muang, Chiang Mai 50200, Thailand

**Abstract** In this paper, CCD photometric light curves for the short-period eclipsing binary 1SWASP J140533.33+114639.1 (hereafter J1405) in the *BVR* bands are presented and analyzed using the 2013 version of the Wilson-Devinney (W-D) code. It is discovered that the J1405 is a W-subtype shallow contact binary with a contact degree of  $f = 7.9 \pm 0.5\%$  and a mass ratio of  $q = 1.55 \pm 0.02$ . In order to explain the asymmetric light curves of the system, a cool star-spot on the more massive component was employed. This shallow contact eclipsing binary may be formed from a short-period detached system through the orbital shrinkage due to angular momentum loss. Based on (*O* – *C*) method, the variation of the orbital period was studied using all the available times of the minimum light. The (*O* – *C*) diagram reveals that the period is increasing continuously at a rate of  $dP/dt = +2.09 \times 10^{-7} \text{ days yr}^{-1}$ , which can be explained by mass transfer from the less massive component to the more massive one.

**Key words:** Stars: binaries: close – Stars: binaries: eclipsing – Stars: individual (1SWASP J140533.33+114639.1).

## 1 INTRODUCTION

The W UMa type contact binaries exhibit a sharp period cutoff phenomenon around 0.22 days (Rucinski 1992). Recent study using the data released by The Large Sky Area Multi-Object Fiber Spectroscopic Telescope (LAMOST) found that new value is around 0.2 days (Qian et al. 2017). The ultrashort-period (less

**Table 1** Coordinates of J1405, the Comparison and Check Stars

Stars	$\alpha_{j2000}$	$\delta_{j2000}$
J1405	$14^h 05^m 33^s .33$	$11^\circ 46' 39'' .1$
Comparison	$14^h 05^m 38^s .23$	$11^\circ 41' 17'' .3$
Check	$14^h 05^m 59^s .16$	$11^\circ 40' 38'' .3$

the distance of stars relying on their empirical period-luminosity relation (Rucinski 2004); (2) these binaries offer significant information about origin and evolution of late-type stars including mass and angular momentum loss, even the merging (Qian et al. 2014; Kjurkchieva et al. 2016). As the development of technology, more and more contact EBs with short-periods were discovered by some Sky Surveys in the world (e.g., SDSS, Super-WASP and NSVS). Till now, some of them have been studied in detail, such as CC Com (Kose et al. 2011; Yang & Liu 2003), GSC1387-475 (Rucinski & Pribulla 2008), 1SWASP J015100.23-100524.2 (Qian et al. 2015a), NSVS 4484038 (Zhang et al. 2014) and the stable red-dwarf contact binary SDSS J001641-000925 (Davenport et al. 2013; Qian et al. 2015b).

1SWASP J140533.33+114639.1 (hereafter J1405) as a short-period contact eclipsing binary (EB) candidate, with a orbital period about 0.225123 days, was first detected in 2013 (Lohr et al. 2013). Its LCs present a typical EW-type (nearly equal light minima). Two Micron All Sky Survey (Cutri et al. 2003) offers its magnitude of  $V=15.51$ ,  $J=14.019$ ,  $H=13.487$  and  $K=13.328$ , and corresponding color index are  $V-K=2.182$ ,  $J-H = 0.532$  and  $H-K = 0.159$  for the system, which imply an average spectral type about K4. However, there is no spectroscopic element, photometric solution or period research published until now. In the present paper, the light curves (LCs) are analyzed using the (W-D) program and its photometric solutions are obtained. All times of minimum light are collected and the period variations are analyzed. The evolutionary scenario and magnetic activity are also discussed.

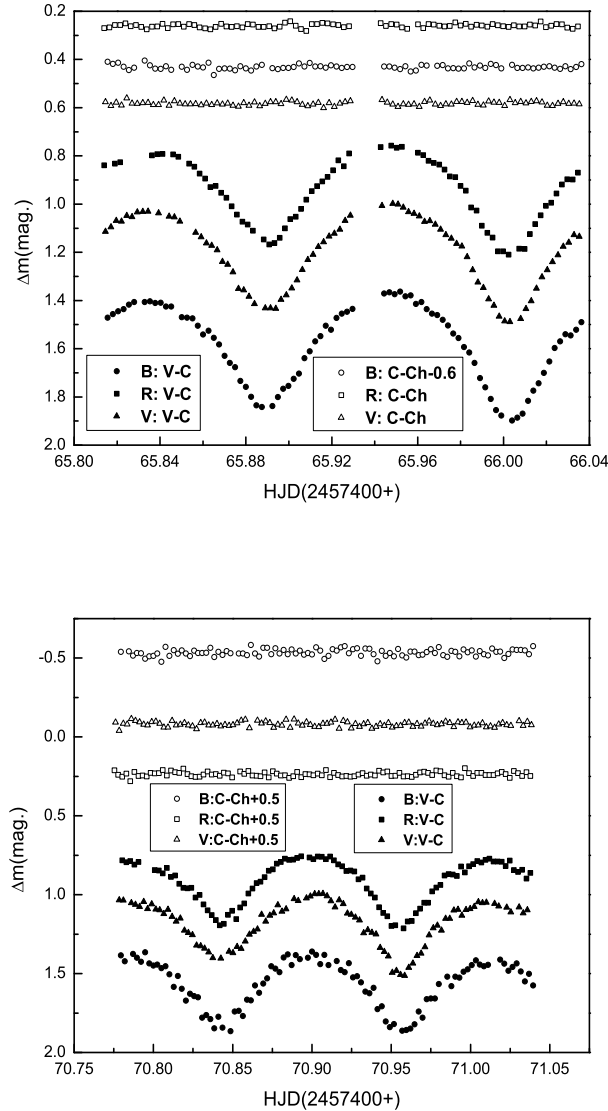
## 2 MULTI-COLOR CCD PHOTOMETRIC OBSERVATIONS

Photometric observations of J1405 were carried out on 2016 March 17 and 22 using the 84 cm telescope at the Observatorio Astronómico Nacional (OAN) at Sierra San Pedro Mártir, Mexico. This relatively small telescope is mainly used for photometric observations, because more than 60% of the nights at this site have photometric quality (Tapia 2003). The integration times for each image in  $BVR$  bands were 70 s, 40 s and 25 s, respectively. All the observed images were reduced using the aperture photometric package PHOT of IRAF by Mr. Michel. Another two stars near the target were chosen as the comparison star and the check star. The coordinates of the variable star, the comparison star and the check star are listed in Table 1. Two sets of LCs obtained are plotted in Figure 1. The LCs are asymmetric and show a weak O'Connell effect (O'Connell 1951), where the maxima following the primary minima are higher than the other maxima. And the average observational errors and the amplitudes of the light variation in different bands are listed in Table 2.

Meanwhile, some new times of light minimum for J1405 were also observed and determined using least-squares parabolic fitting method. By use of the following linear ephemeris:

**Table 2** The Average Observational Errors and the Amplitudes of the Light Variation in March 2016

Band	Date	Error(.mag)	$\Delta m$ (.mag)	Date	Error(.mag)	$\Delta m$ (.mag)
B	17	0.0071	0.5852	22	0.0102	0.6646
V	17	0.0071	0.5231	22	0.0087	0.5592
R	17	0.0067	0.5480	22	0.0081	0.5303

**Fig. 1** The observational LCs of J1405 in *BVR* bands. The differential light curves of the comparison star relative to the check star are also plotted.

the  $(O - C)$  values and observational LCs' phase were calculated. The zeropoint displayed in this linear ephemeris was one of primary eclipse times, which was determined using the observed data from 84 cm telescope, and the orbital period we adopted came from Super-WASP EB catalog (Lohr et al. 2013). All the

**Table 3** (O-C) Values of Light Minima for J1405

HJD(2450000+)	(O-C)	E	Filter	Telescope	HJD(2450000+)	(O-C)	E	Filter	Telescope	HJD(2450000+)	(O-C)	E	Filter	Telescope
7465.8895(02)	-0.0009	-0.5	<i>BVR</i>	84 cm	4941.4512(46)	-0.0224	-11214	<i>V</i>	INGT	5279.5906(0.40)	-0.0178	-9712	<i>V</i>	INGT
7466.0029(02)	0.0000	0	<i>BVR</i>	84 cm	4942.5783(57)	-0.0209	-11209	<i>V</i>	INGT	5280.4858(0.49)	-0.0230	-9708	<i>V</i>	INGT
7470.8427(08)	-0.0004	21.5	<i>BVR</i>	84 cm	4943.4743(43)	-0.0254	-11205	<i>V</i>	INGT	5281.6167(0.65)	-0.0178	-9703	<i>V</i>	INGT
7470.9563(06)	0.0006	22	<i>BVR</i>	84 cm	4944.6026(31)	-0.0228	-11200	<i>V</i>	INGT	5290.6089(0.50)	-0.0305	-9663	<i>V</i>	INGT
4450.0010(...)	-0.0291	-13397	<i>V</i>	INGT	4945.5019(30)	-0.0239	-11196	<i>V</i>	INGT	5291.5206(0.44)	-0.0193	-9659	<i>V</i>	INGT
4530.6109(42)	-0.0132	-13039	<i>V</i>	INGT	4949.5605(34)	-0.0175	-11178	<i>V</i>	INGT	5292.6417(0.42)	-0.0238	-9654	<i>V</i>	INGT
4532.6232(26)	-0.0271	-13030	<i>V</i>	INGT	4950.4561(26)	-0.0224	-11174	<i>V</i>	INGT	5293.5505(0.36)	-0.0155	-9650	<i>V</i>	INGT
4533.5289(49)	-0.0218	-13026	<i>V</i>	INGT	4955.6460(73)	-0.0104	-11151	<i>V</i>	INGT	5294.6693(0.24)	-0.0223	-9645	<i>V</i>	INGT
4535.5631(35)	-0.0138	-13017	<i>V</i>	INGT	4963.5170(47)	-0.0187	-11116	<i>V</i>	INGT	5295.5787(0.37)	-0.0134	-9641	<i>V</i>	INGT
4536.4510(35)	-0.0263	-13013	<i>V</i>	INGT	4964.6351(39)	-0.0262	-11111	<i>V</i>	INGT	5297.5974(0.49)	-0.0208	-9632	<i>V</i>	INGT
4539.6050(50)	-0.0241	-12999	<i>V</i>	INGT	4965.5461(59)	-0.0157	-11107	<i>V</i>	INGT	5298.4989(0.32)	-0.0198	-9628	<i>V</i>	INGT
4555.5957(21)	-0.0171	-12928	<i>V</i>	INGT	4966.6605(48)	-0.0269	-11102	<i>V</i>	INGT	5304.5789(0.41)	-0.0181	-9601	<i>V</i>	INGT
4558.5209(50)	-0.0185	-12915	<i>V</i>	INGT	4967.5715(48)	-0.0164	-11098	<i>V</i>	INGT	5307.4995(0.37)	-0.0241	-9588	<i>V</i>	INGT
4573.6128(78)	-0.0098	-12848	<i>V</i>	INGT	4968.4678(39)	-0.0205	-11094	<i>V</i>	INGT	5308.6352(0.48)	-0.0140	-9583	<i>V</i>	INGT
4591.6039(32)	-0.0286	-12768	<i>V</i>	INGT	4969.5905(47)	-0.0235	-11089	<i>V</i>	INGT	5309.5267(0.51)	-0.0230	-9579	<i>V</i>	INGT
4593.6353(27)	-0.0233	-12759	<i>V</i>	INGT	4970.4921(36)	-0.0224	-11085	<i>V</i>	INGT	5318.5369(0.82)	-0.0178	-9539	<i>V</i>	INGT
4596.5626(37)	-0.0226	-12746	<i>V</i>	INGT	4971.6100(37)	-0.0301	-11080	<i>V</i>	INGT	5319.6648(0.37)	-0.0155	-9534	<i>V</i>	INGT
4597.4642(43)	-0.0214	-12742	<i>V</i>	INGT	4972.5159(55)	-0.0247	-11076	<i>V</i>	INGT	5321.4552(0.36)	-0.0260	-9526	<i>V</i>	INGT
4598.5876(41)	-0.0237	-12737	<i>V</i>	INGT	4973.6431(43)	-0.0232	-11071	<i>V</i>	INGT	5322.5825(0.36)	-0.0243	-9521	<i>V</i>	INGT
4608.5046(74)	-0.0121	-12693	<i>V</i>	INGT	4974.5450(49)	-0.0217	-11067	<i>V</i>	INGT	5324.6152(0.42)	-0.0177	-9512	<i>V</i>	INGT
4609.6179(76)	-0.0244	-12688	<i>V</i>	INGT	4975.6699(22)	-0.0224	-11062	<i>V</i>	INGT	5331.5982(0.37)	-0.0136	-9481	<i>V</i>	INGT
4611.6472(33)	-0.0212	-12679	<i>V</i>	INGT	4976.5682(57)	-0.0247	-11058	<i>V</i>	INGT	5333.6231(0.54)	-0.0147	-9472	<i>V</i>	INGT
4613.6671(69)	-0.0274	-12670	<i>V</i>	INGT	4977.4694(50)	-0.0239	-11054	<i>V</i>	INGT	5334.5176(0.35)	-0.0207	-9468	<i>V</i>	INGT
4614.5766(69)	-0.0184	-12666	<i>V</i>	INGT	4978.5984(58)	-0.0205	-11049	<i>V</i>	INGT	5335.6492(0.41)	-0.0147	-9463	<i>V</i>	INGT
4615.4670(77)	-0.0286	-12662	<i>V</i>	INGT	4979.4993(52)	-0.0201	-11045	<i>V</i>	INGT	5336.5411(0.36)	-0.0234	-9459	<i>V</i>	INGT
4619.5244(84)	-0.0233	-12644	<i>V</i>	INGT	4980.6185(36)	-0.0265	-11040	<i>V</i>	INGT	5337.6671(0.52)	-0.0230	-9454	<i>V</i>	INGT
4620.6515(43)	-0.0218	-12639	<i>V</i>	INGT	4981.5197(53)	-0.0258	-11036	<i>V</i>	INGT	5343.5241(0.63)	-0.0192	-9428	<i>V</i>	INGT
4896.6416(41)	-0.0326	-11413	<i>V</i>	INGT	4982.6499(35)	-0.0213	-11031	<i>V</i>	INGT	5348.4781(0.39)	-0.0179	-9406	<i>V</i>	INGT
4910.6146(40)	-0.0172	-11351	<i>V</i>	INGT	4983.5402(65)	-0.0314	-11027	<i>V</i>	INGT	5350.5047(0.47)	-0.0174	-9397	<i>V</i>	INGT
4912.6332(34)	-0.0247	-11342	<i>V</i>	INGT	5240.6413(47)	-0.0208	-9885	<i>V</i>	INGT	5617.5019(0.78)	-0.0161	-8211	<i>V</i>	INGT
4913.5382(32)	-0.0202	-11338	<i>V</i>	INGT	5249.6515(66)	-0.0155	-9845	<i>V</i>	INGT	5618.6192(0.62)	-0.0244	-8206	<i>V</i>	INGT
4919.6161(47)	-0.0206	-11311	<i>V</i>	INGT	5265.6296(35)	-0.0212	-9774	<i>V</i>	INGT	5619.5208(0.57)	-0.0232	-8202	<i>V</i>	INGT
4921.6366(32)	-0.0262	-11302	<i>V</i>	INGT	5267.6546(35)	-0.0223	-9765	<i>V</i>	INGT	5620.6495(0.27)	-0.0202	-8197	<i>V</i>	INGT
4923.6640(38)	-0.0249	-11293	<i>V</i>	INGT	5268.5603(32)	-0.0170	-9761	<i>V</i>	INGT	5621.5492(0.39)	-0.0210	-8193	<i>V</i>	INGT
4924.5722(59)	-0.0172	-11289	<i>V</i>	INGT	5269.4593(62)	-0.0185	-9757	<i>V</i>	INGT	5622.6737(0.34)	-0.0221	-8188	<i>V</i>	INGT
4925.4686(53)	-0.0213	-11285	<i>V</i>	INGT	5270.5812(39)	-0.0223	-9752	<i>V</i>	INGT	5623.5817(0.62)	-0.0146	-8184	<i>V</i>	INGT
4926.5957(39)	-0.0198	-11280	<i>V</i>	INGT	5271.4820(59)	-0.0219	-9748	<i>V</i>	INGT	5646.5382(0.54)	-0.0206	-8082	<i>V</i>	INGT
4927.4840(43)	-0.0320	-11276	<i>V</i>	INGT	5272.6103(38)	-0.0193	-9743	<i>V</i>	INGT	5647.6642(0.40)	-0.0202	-8077	<i>V</i>	INGT
4935.6006(39)	-0.0198	-11240	<i>V</i>	INGT	5273.5063(61)	-0.0238	-9739	<i>V</i>	INGT	5648.5741(0.51)	-0.0109	-8073	<i>V</i>	INGT
4936.4974(38)	-0.0235	-11236	<i>V</i>	INGT	5275.5328(48)	-0.0234	-9730	<i>V</i>	INGT	5649.4581(0.52)	-0.0274	-8069	<i>V</i>	INGT
4938.5190(33)	-0.0280	-11227	<i>V</i>	INGT	5276.6617(39)	-0.0200	-9725	<i>V</i>	INGT	6736.7630(0.02)	0.0460	-3239.5	<i>V</i>	INGT
4939.6506(34)	-0.0220	-11222	<i>V</i>	INGT	5277.5637(55)	-0.0185	-9721	<i>V</i>	INGT	6736.8722(0.03)	0.0426	-3239	<i>V</i>	INGT
4940.5518(40)	-0.0213	-11218	<i>V</i>	INGT	5278.4612(31)	-0.0215	-9717	<i>V</i>	INGT					

Ref: INGT means Isaac Newton Group of Telescopes, Apartado de Correos 321, E-38700 Santa Cruz de La Palma, Tenerife, Spain.

### 3 ORBITAL PERIOD INVESTIGATION

The ( $O - C$ ) method is the traditional way to reveal variations on orbital period. Before the present work, only one minima time of J1405 had been published. For analysing the period changes of the system, we

!h

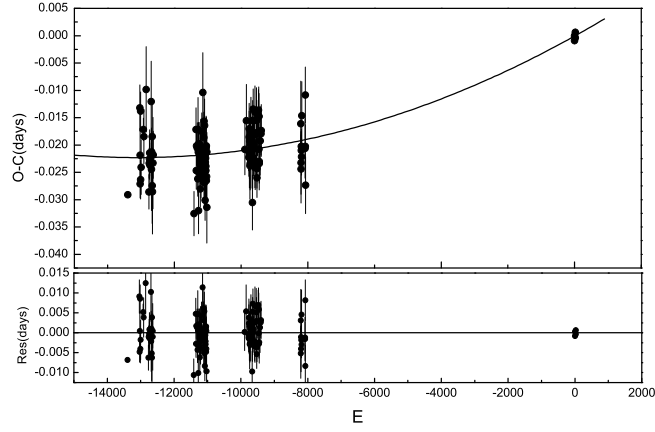


**Fig. 2** The  $(O-C)$  diagram of J1405 formed by all available measurements. The  $(O-C)$  values were computed by using a newly determined linear ephemeris (Eq.1). The solid line represents the quadratic fit (Eq.2). The bottom panel plots the residuals for Equation 2.

WASP, and the LCs obtained from OAN offered another 4. Minimum times with the same epoch have been averaged, and only the mean values are listed in Table 3. In our fitting process, according to determined errors listed in Table 3, the weight of the Super WASP data is 1 and that of our data is 5.

The  $(O-C)$  diagram shows an upward parabola variation and the fitting curve is plotted in Figure 2. Based on the least-square method, the new ephemeris

$$\begin{aligned}
 \text{Min. I} &= 2457470.95618(\pm 0.0003) \\
 &+ 0.^d22512639(\pm 0.00000003) \times E \\
 &+ 1.29(\pm 0.02) \times 10^{-10} \times E^2
 \end{aligned}
 \tag{2}$$

was obtained. With the quadratic term included in this equation, a secular period increase rate is determined:  $dP/dt = 2.09 \times 10^{-7} \text{ days yr}^{-1}$ .

#### 4 PHOTOMETRIC SOLUTIONS

To derive its physical parameters, the 2013 version of Wilson-Devinney (W-D) program (Wilson 1971; Wilson & Van 2003; Wilson et al. 2010) is used. The number of observational data applied in the program are 81 in  $B$  band, 78 in  $V$  band, and 72 in  $R$  band.

Before analyzing the LCs, the value of some input parameter were set. The temperature for star 1 (star eclipsed at the primary light minimum),  $T_1 = 4680K$  was fixed according to mean color index (Cox 2000).

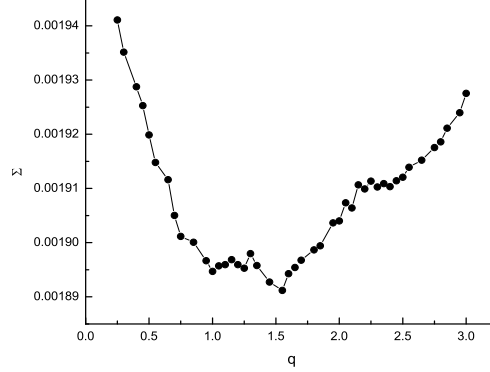


**Fig. 3** The  $\Sigma - q$  curve for J1405. The minimum residuals is at  $q = 1.55$ .

i.e.,  $g_1 = g_2 = 0.32$  according to the stellar temperatures given by Claret (2000) and  $A_1 = A_2 = 0.5$  (Lu & Rucinski 1993) were set for late-type stars with a convective envelope. The bolometric and bandpass limb-darkening coefficients were chosen from Van Hamme (1993). To account for the limb-darkening in detail, logarithmic functions are used. These fixed parameters are listed in Table 4. The adjustable parameters were: the mass ratio,  $q$ ; the orbital inclination,  $i$ ; the mean temperature of star 2,  $T_2$ ; the dimensionless potentials of the two components  $\Omega_1$  and  $\Omega_2$ ; the monochromatic light of star 1,  $L_{1B}$ ,  $L_{1V}$ , and  $L_{1R}$ .

Two sets of LCs are obtained, but, the data from March 17 are of better quality. So, we started the analysis with this set of LCs. Mode 3 for contact binary system is adopted ( $\Omega_1 = \Omega_2$  in this case). Because there is no spectroscopic observations for J1405 published, we used a  $q$ -search method (fix  $q$ ) to obtain initial input parameters. The solutions are carried out with mass ratios ranging from less than 0.25 to larger than 3.0. The relation between the sum of weighted square deviations  $\Sigma\omega(O-C)^2$  and  $q$  is plotted in Figure 3. The  $\Sigma - q$  curves shown a lowest value at  $q = 1.55$ . We then set the initial value of  $q$  to be 1.55 and treated it as an adjustable parameter. After all the free parameters converged, one set of solutions was derived. Because our LCs are asymmetric, and the main reason is the variation of spot location and size (Kang et al. 2002). Considering this case, cool star-spots model was used to get better solutions. As we all know, four parameters to describe a spot, namely the temperature factor,  $T_s$ ; the latitude,  $Lat$ ; the longitude  $Lon$  and the angular radius  $Rad$ . During our analysis, only the  $T_s$  was fixed at a series of trial values until we found the best solution. Finally, we found that one cool star-spot on the secondary component could get the best fit, and the fitting residual of our solution with spot is much smaller than that without spot. Therefore, we adopted the cool star-spot model as the final solution. The derived photometric solutions are listed in the Table 5 and the theoretical LCs computed with the cool star-spot model are plotted in the Figure 4. Besides, we also get the geometrical structure of the system, which is shown in Figure 5. Because the LCs obtained on March 22 are of worse quality, and we didn't analyze them.

## 5 DISCUSSIONS AND CONCLUSIONS

The asymmetry displayed by the observed LCs suggests a spot activity of the system. Because of that, we

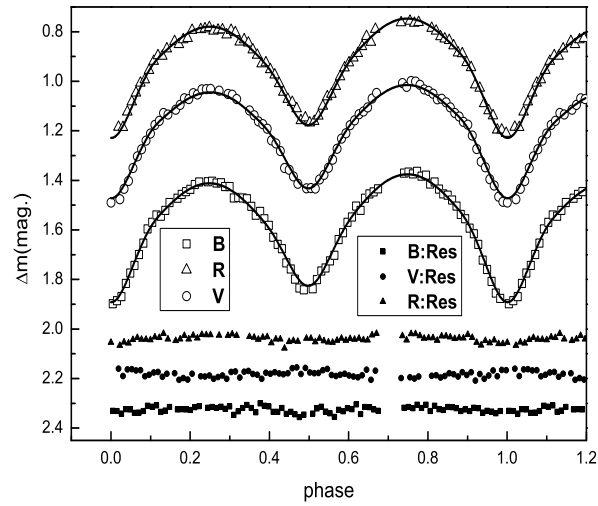


**Fig. 4** Observed (open cycle, triangle and square) and theoretical light curves (solid line) calculated with cool star-spot listed in Table 5. Residuals from the solutions are shown in the bottom panel.

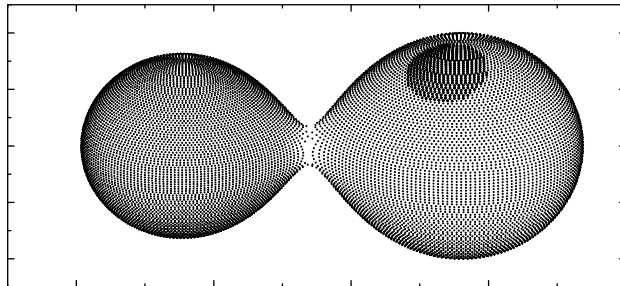


**Fig. 5** Geometric structure of J1405 at phase 0.25.

ponent using the 2013 version of the Wilson-Devinney code. The results suggest that J1405 is a W-subtype contact eclipsing binary near the short-period cutoff with a mass ratio of  $q = 1.55 \pm 0.02$ . The mean contact degree ( $f = 7.3\%$ ) reveals that it is a shallow contact system with similar surface temperature of the components ( $\Delta T = 140K$ ). Similar contact binaries including AH Vir (Lu & Rucinski 1993; Kjurkchieva et al. 2015), RZ Com (He & Qian 2008; Xiang & Zhou 2004), AM Leo (Hille et al. 2004), U Peg (Mohajerani

**Table 4** Fixed Parameters During Photometric Analysis

Parameters	Values
$g_1 = g_2$	0.32
$A_1 = A_2$	0.50
$x_{1bolo}, x_{2bolo}$	0.641, 0.638
$y_{1bolo}, y_{2bolo}$	0.172, 0.163
$x_{1B}, x_{2B}$	0.848, 0.844
$y_{1B}, y_{2B}$	0.096, 0.129
$x_{1V}, x_{2V}$	0.802, 0.801
$y_{1V}, y_{2V}$	0.045, 0.022
$x_{1R}, x_{2R}$	0.749, 0.755
$y_{1R}, y_{2R}$	0.123, 0.108

**Table 5** Photometric Solutions for J1405

Parameters	March 17th		March 17th	
	No spot	Errors	With spot	Errors
$T_1(K)$	4680	Assumed	4680	Assumed
$q$	1.5501	$\pm 0.0199$	1.5488	$\pm 0.0163$
$T_2(K)$	4563	$\pm 16$	4523	$\pm 21$
$i(^{\circ})$	68.996	$\pm 0.257$	68.616	$\pm 0.321$
$L_1/(L_1 + L_2)(B)$	0.4545	$\pm 0.0074$	0.4742	$\pm 0.0135$
$L_1/(L_1 + L_2)(V)$	0.4434	$\pm 0.0058$	0.4590	$\pm 0.0121$
$L_1/(L_1 + L_2)(R)$	0.4342	$\pm 0.0045$	0.4466	$\pm 0.0112$
$\Omega_1 = \Omega_2$	4.5612	$\pm 0.0092$	4.5528	$\pm 0.0026$
$r_1(pole)$	0.3237	$\pm 0.0009$	0.3247	$\pm 0.0011$
$r_1(side)$	0.3391	$\pm 0.0011$	0.3402	$\pm 0.0015$
$r_1(back)$	0.3733	$\pm 0.0016$	0.3751	$\pm 0.0022$
$r_2(pole)$	0.3967	$\pm 0.0009$	0.3976	$\pm 0.0014$
$r_2(side)$	0.4201	$\pm 0.0011$	0.4213	$\pm 0.0018$
$r_2(back)$	0.4510	$\pm 0.0015$	0.4526	$\pm 0.0025$
$f(\%)$	6.7	$\pm 1.6$	7.9	$\pm 0.5$
Latitude( $^{\circ}$ )			334.392	$\pm 4.242$
Longitude( $^{\circ}$ )			253.902	$\pm 6.187$
Radius(radian)			0.356	$\pm 0.089$
$T_s$			0.85	Assumed
$\sum \omega_i(O - C)_i^2$	0.001891		0.001135	

from initially detached binaries by angular momentum loss (AML) via magnetic braking (Qian et al. 2013). As other late K-type contact binaries with the short-period, J1405 is also in marginal contact and presents remarkable asymmetric light curves, representing probable surface activities (Zhang et al. 2014; Jiang et al. 2015a). Just as Qian et al. (2015a) discussed, the orbital shrinkage due to AML may result in the formation of a contact system similar to J1405. The progenitor of J1405 may be a short-period detached EB system similar to DV Psc (Pi et al. 2014), and the J1405 may be at the same evolutionary phase like the 1SWASP



Another feature of J1405 is its spot activity. Generally, for late-type contact binary stars, their deep convective envelope along with fast rotation can help to produce a strong magnetic dynamo, because of that, they will display some solar-like activity such as photospheric cool star-spots (Li et al. 2015). A cool star-spot is known as the strong magnetic area which can change the shape of LCs. We adopted cool star-spot model of the (W-D) program with one spot on the secondary component to explain it. Just as the Figure 4 shown, the fitting LCs with cool star-spot coincide very well with the observational data at all phases. Therefore, using cool star-spot model to explain the asymmetry of LCs are reasonable.

Based on the analysis of the ( $O - C$ ) diagram, we found that the orbital period of J1405 show a upward parabolic variation, which represents an increase of the period. According to the obtained parameters, the rate of  $dP/dt=2.09 \times 10^{-7} \text{days yr}^{-1}$  is derived. The secular increase of the orbital period may be interpreted as the mass transfer from the less massive component to the more massive one, such as EP And (Liao et al. 2013), 1SWASP J074658.62+224448.5 (Jiang et al. 2015a), 1SWASP J075102.16+342405.3 (Jiang et al. 2015b). However, the time span of our data is only 10 years, the increase of the period might be only a part of long-term changes. Further observations are required to confirm this result.

**Acknowledgements** This work is partly supported by Chinese Natural Science Foundation (No.11133007, 11573063), the Science Foundation of Yunnan Province (grant No. 2012HC011). Many thanks to Dr.Marcus Lohr for his kindly sending us eclipse timings of J1405. We are also especially indebted to the anonymous referees who given us useful comments and cordial suggestions, which helped us to improve the paper greatly.

## References

- Chen, M., Xiang, F. Y., Yu, Y. X. & Xiao, T. Y. 2015, *Research in Astron. Astrophys. (RAA)*, 9, 349
- O'Connell, D. J. K. 1951, *MNRAS*, 111, 642
- Cox, A. N. 2000, *Allens Astrophysical Quantities* (4th ed.; New York: Springer)
- Cutri, R. M., Skrutskie, M. F., et al. 2003, *VizieR Online Data Catalog*, 2246, 0
- Davenport, James R. A., et al. 2013, *ApJ*, 764, 62
- Djurašević, G., et al. 2001, *A&A*, 367, 840
- He, J. J. & Qian, S. B. 2008, *CHJAA*, 8, 465
- Hiller, M. E., Osborn, W. & Terrell, D. 2004, *PASP*, 116, 337
- Jiang, L. Q., Qian, S. B., et al. 2015, *AJ*, 149, 169
- Jiang, L. Q., et al. 2015, *PASJ*, 149, 169
- Kang, Y. W., Oh, K. D., Kim, C. H. et al. 2002, *MNRAS*, 331, 707
- Kjurkchieva, D. P., Dimitrov, D. P. & Ibryamov, S. I. 2015, *Research in Astron. Astrophys. (RAA)*, 15, 1493
- Kjurkchieva, D., Popov, V., Vasileva, D. & Petrov, N. 2016, *SerAJ*, 192, 21
- Kose, O., et al. 2011, *AN*, 332, 626
- Li, K., Hu, S. M., Guo, D. F., et al. 2015, *AJ*, 149, 120
- Liao, W. P., et al. 2013, *AJ*, 146, 79
- Liu, N. P., et al. 2015, *AJ*, 149, 148
- Lohr, M. E., et al. 2013, *A&A*, 549, 86
- Lohr, M. E., Hodgkin, S. T., et al. 2014, *A&A*, 563, 34
- Lu, W. X & Rucinski, S. M. 1993, *AJ*, 106, 361
- Mohajerani, S & Percy, J. R. 2011, *JAVSO*, 563, 34
- Norton, A. J., et al. 2011, *A&A*, 528, 90
- Pi, Q. F., Zhang, L. Y., et al. 2014, *AJ*, 147, 50
- Qian, S. B., Liu, N. P., Li, K., et al. 2013, *ApJS*, 209, 13

- Qian, S. B., Zhang, B., et al. 2015a, *AJ*, 150, 117
- Qian, S. B., Jiang, L. Q., et al. 2015b, *ApJ*, 798, 42
- Qian, S. B., He, J. J., et al. 2017, *Research in Astron. Astrophys. (RAA)*, 17, 87
- Rucinski, S. M. 1992, *AJ*, 103, 960
- Rucinski, S. M. 2004, *NewAR*, 48, 703
- Rucinski, S. M., Pribulla, T. 2008, *MNRAS*, 388, 1831
- Şenavcı, H. V. 2012, *IAUS*, 282, 496
- Tapia, M. 2003, *RMxAC*, 19, 75
- Wilson, R. E. & Devinney, E. J. 1971, *ApJ*, 166, 605
- Wilson, R. E. & Van Hamme, W. 2003, *Computing Binary Stars Observables*, the 4th edition of the W-D programe.
- Wilson, R. E., Van, Hamme. W. & Terrell, D., 2010, *ApJ*, 723, 1469
- Van Hamme, W. 1993, *AJ*, 106, 2096
- Xiang, F. Y. & Zhou, Y. C. 2004, *NewA*, 9, 273
- Yang, Y. L. & Liu, Q. Y. 2003, *PASP*, 115, 748
- Zhang, X. B., Deng, L. C., et al. 2014, *AJ*, 148, 40
-